Engineering Geology 332 (2024) 107477

Contents lists available at ScienceDirect

Engineering Geology

journal homepage: www.elsevier.com/locate/enggeo

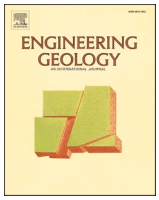

Case study of a foundation failure induced by cyclic softening of clay during the 2023 Kahramanmaraş earthquakes

İ. Tonyalı [a], S.O. Akbas [a,*], T. Beyaz [b], K. Kayabalı [c], C. Gokceoglu [d]

[a] Civil Eng. Dept., Gazi Univ., Maltepe, Ankara 06570, Turkey
[b] Geological Eng. Dept., Pamukkale Univ., Denizli, Turkey
[c] Geological Eng. Dept., Ankara Univ., Ankara, Turkey
[d] Geological Eng. Dept., Hacettepe Univ., Ankara, Turkey

ARTICLE INFO

Keywords:
Kahramanmaraş earthquakes
Cyclic softening
Bearing capacity
Clay

ABSTRACT

The Kahramanmaraş Earthquakes that occurred on 6 February 2023 resulted in extensive structural failures, including damages caused by soil liquefaction. This study focused on investigating the excessive settlements observed in buildings along Ataturk Boulevard in the Golbasi district, with a primary emphasis on the toppling failure of the Kayı Apartment. Field exploration, laboratory testing, and bearing capacity analyses were conducted to understand the failure mechanism. Since the foundation soil of Kayı Apartment predominantly consisted of clay, soil liquefaction alone could not explain the observed failure. Instead, the cyclic softening of clayey soil underground shaking was identified as a significant factor contributing to the damage. As one of the rare case histories documenting a failure caused by cyclic softening, the results of the study also shed light on the excessive displacements observed in nearby buildings with fewer stories that managed to withstand the earthquake without experiencing complete bearing capacity failure.

1. Introduction

Two destructive earthquakes with magnitudes of 7.7 and 7.6 M_w, respectively, occurred nine hours apart on February 6, 2023, with their epicenters in the Pazarcık and Elbistan districts of Kahramanmaraş, resulting in the loss of 59,000 lives and over 122,000 injuries in Turkey and Syria. Following the earthquakes, over 30,000 aftershocks measuring up to 6.7 M_w were recorded.

The earthquakes occurred near the triple junction of the Anatolian, Arabian, and African plates and were felt in a wide geographic region that includes Lebanon, Cyprus, Iraq, Israel, Jordan, Iran, and Egypt, causing damage in an area of approximately 350,000 km^2. In Turkey, the earthquakes affected approximately 14 million people in the provinces of Kahramanmaraş, Hatay, Gaziantep, Şanlıurfa, Osmaniye, Malatya, Kilis, Adıyaman, Diyarbakır, Elazığ, and Adana.

As of March 6, 2023, the Ministry of Environment, Urbanization and Climate Change (ÇŞİDB) in Turkey has evaluated the damage caused by the earthquake in 11 provinces on a total of 1,712,182 buildings. The data indicates that 35,355 buildings collapsed, while 17,491 require immediate demolition. Moreover, 179,786 buildings are classified as heavily damaged, 40,228 as moderately damaged, and 431,421 as slightly damaged. It is worth mentioning that the damaged buildings include not only residential structures, but also culturally and historically significant buildings, as well as schools, administrative buildings, hospitals, and hotels.

Soil liquefaction caused extensive damage in many portions of the affected area. Structures on saturated river deposits as well as in coastal areas that include port facilities, buildings, bridges, and lifelines experienced significant liquefaction-induced damage. In areas where soil failures or liquefaction took place, it was observed that a significant number of buildings that had not sustained any structural damage sunk into the soil or tilted as a rigid unit as a result of excessive uniform or differential settlements.

Soil liquefaction was believed to be responsible for the extensive settlements and tilting observed at buildings on Atatürk Boulevard in Gölbaşı district, especially the phenomenal failure of the Kayı Apartment. However, it may not be the appropriate explanation for this failure, since the mat foundation of the Kayı Apartment was settled primarily on clayey soil as the borings conducted right after the earthquakes indicated. Instead, the damage could have been induced by the

* Corresponding author.
E-mail addresses: ilkay.tonyali@gazi.edu.tr (İ. Tonyalı), soakbas@gazi.edu.tr (S.O. Akbas), tbeyaz@pau.edu.tr (T. Beyaz), kayabali@ankara.edu.tr (K. Kayabalı), cgokce@hacettepe.edu.tr (C. Gokceoglu).

https://doi.org/10.1016/j.enggeo.2024.107477
Received 16 November 2023; Received in revised form 5 March 2024; Accepted 11 March 2024
Available online 12 March 2024
0013-7952/© 2024 Elsevier B.V. All rights reserved.

cyclic softening of the clayey soil due to ground shaking.

In areas where low-plasticity clayey soils are present, the occurrence of ground failure and building settlement during earthquakes has presented intriguing cases of damage, particularly as observed in the 1999 Chi-Chi, Taiwan earthquake (Chu et al., 2008). Another noteworthy event, the 1999 Kocaeli earthquake, involved in-situ deformation measurements at the Carrefour Shopping Center, revealing significant vertical strains within the clay layer, leading Martin et al. (2004) to classify its behavior as "resembling liquefaction". Tsai and Hashash (2009) further investigated the degradation behavior of soils, noting that sandy soil exhibits more pronounced degradation compared to clayey soil.

In the literature, it is possible to find several studies performed on liquefaction (i.e. Gratchev et al., 2006; Kayabasi and Gokceoglu, 2018; Xu et al., 2020). However, despite cyclic softening being a well-recognized response of clay under cyclic loading, there exists a scarcity of well-documented case histories compared to those focusing on soil liquefaction. The Rixin levee failure following the Meinong earthquake, attributed to cyclic degradation as recently identified by Tsai et al. (2022), underscores the critical need for additional case studies to illustrate occurrences of cyclic softening. Such efforts are essential for researchers to validate their models and analysis procedures effectively. It is evident that the well documented case histories may help for development of earthquake resistant designs to be constructed on clayey soils.

The objective of this research is to document and investigate the excessive deformations experienced by buildings on Atatürk Boulevard in Gölbaşı district, focusing mainly on the failure of Kayı Apartment, with a specific focus on understanding the underlying mechanism of cyclic softening. The failure was initially identified and reported as liquefaction-induced during the preliminary assessments and reconnaissance studies conducted immediately after the Kahramanmaraş earthquakes. Subsequently, field investigations and laboratory studies including dynamic shear tests were conducted to characterize the foundation soil. Based on the gathered data, a comprehensive analysis was carried out, encompassing liquefaction potential and the resulting bearing capacity. Notably, the analysis incorporated the consideration of cyclic softening in the clayey soil subjected to cyclic loading.

2. Description of the observed damage

The study area is located in the Gölbaşı district, which is situated on the Gaziantep-Malatya highway and the Adana-Malatya railway route, connecting the Eastern Mediterranean and Southeastern Anatolia regions to Eastern Anatolia. The Gölbaşı district is 62 km away from Adıyaman, 105 km from Malatya, 100 km from Kahramanmaraş, and 122 km from Gaziantep (Fig. 1). The town, which is situated adjacent to the tectonic Golbasi lake, lies on the Gölbaşı-Türkoğlu fault segment, which is part of the Eastern Anatolian Fault Zone (EAFZ) as defined by Şaroğlu et al. (1987).

The shakemap PGA contours for the M 7.7 Kahramanmaraş Earthquake are shown in Fig. 2 with a maximum peak ground acceleration (PGA) recorded as 1.057 g. According to Fig. 2, the PGA experienced in Gölbaşı was between 0.2 g and 0.3 g. Regrettably, although the earthquakes generated a large number of ground-motion recordings, there were no usable recordings available in the vicinity of Gölbaşı, during the M_w 7.7 and M_w 7.6 events. Based on the widely-used attenuation relationships, it is estimated that the peak horizontal ground acceleration at the Kayı Apartment site, located 70 km from the fault rupture, would have been approximately 0.20 g on a hypothetical 'rock outcrop' and 0.25 g on soft soil. This estimation aligns with the simplified one-dimensional equivalent linear site response studies, which indicate a range of 0.20–0.30 g for the peak horizontal ground acceleration at the site. The observed damage levels to the buildings further corroborate this conclusion. Thus, for the purposes of analyses conducted herein, the PGA for Kayı Apartment site was taken to be between 0.2 g and 0.3 g.

In Gölbaşı, about 60% of the buildings in the city center collapsed during the two earthquakes, while the remaining structures suffered heavy damage. Almost every building near Gölbaşı lake experienced ground displacements and deformations, such as settlement and lateral spreading, due to liquefaction. It was originally reported that seismic soil liquefaction also caused some residential buildings to lose their bearing capacity, resulting in tilted and overturned structures. Additionally, it has been observed that the occurrence of bearing capacity failure and excessive settlements are more prominent in buildings with five to seven stories compared to those consisting of one to three stories (EERI, 2023).

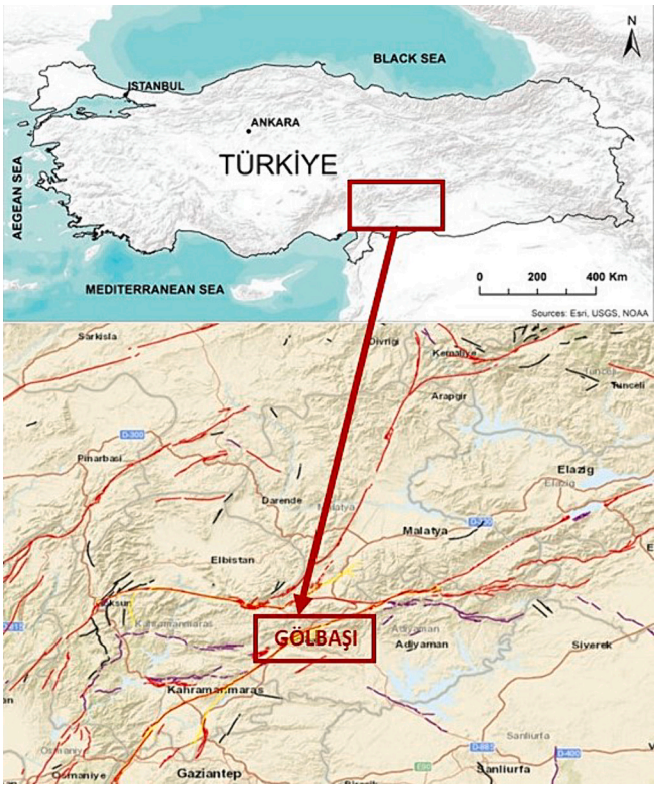

Fig. 1. Location Map of Gölbaşı district (www://yerbilimleri.mta.gov.tr).

Through a preliminary investigation, data was collected for 12 structures situated along a 250-m segment of Atatürk Boulevard, which runs parallel to the Gölbaşı Lake, in order to assess the horizontal and vertical deformations caused by earthquakes (Fig. 3). The settlements observed in the structures are presented in Table 1. One of the most remarkable structures in this region is the Kayı Apartment, a 6-story building located on Parcel 11 of Ataturk Boulevard, which is noteworthy for its intriguing characteristic of toppling over without exhibiting any observable structural damage (Fig. 4). The failure mechanism observed in this case differed from the typical excessive deformations commonly observed elsewhere, resembling more of a bearing capacity failure. It remained unclear whether the failure was attributed to liquefaction or not based solely on the observed mode of failure, especially without credible subsurface geotechnical characterization.

The building rests on a reinforced concrete mat foundation with dimensions of 11 m × 24 m at a depth of about 1.2 m. A model of the six-story reinforced concrete structure was prepared to estimate the bearing pressures on the mat foundation as shown in Fig. 5.

There was no indication of a significant amount of soil bulging or mound formation around the structure, suggesting that the failure surface was not well-defined and did not extend to the ground surface. This observation indicates that the failure occurred progressively, with a continuous downward movement or punching of the foundation. Punching shear failures are more likely to occur in soils that exhibit a very plastic type of load-settlement behavior. Therefore, the lack of

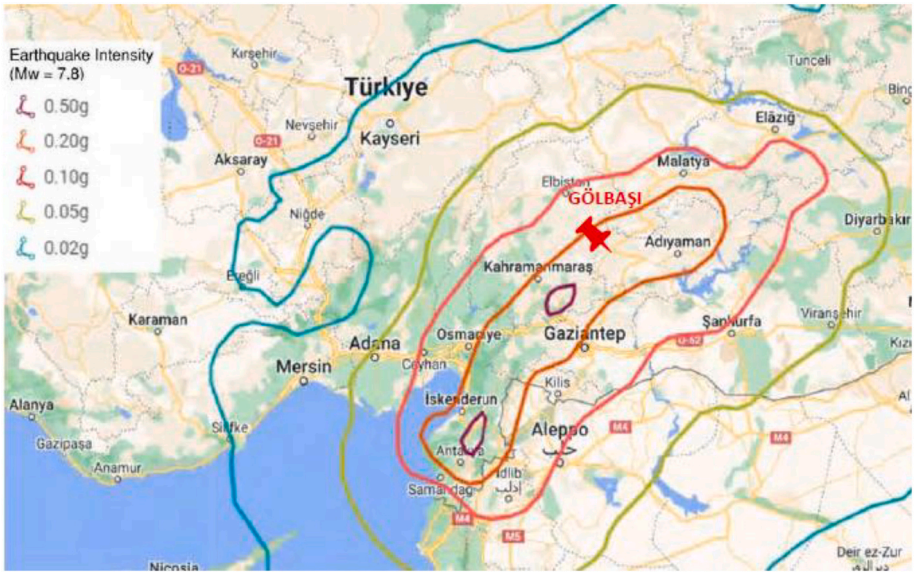

Fig. 2. Shakemap PGA contours for the M 7.7 Kahramanmaraş Earthquake (Source: https://earthquake.usgs.gov/earthquakes/eventpage).

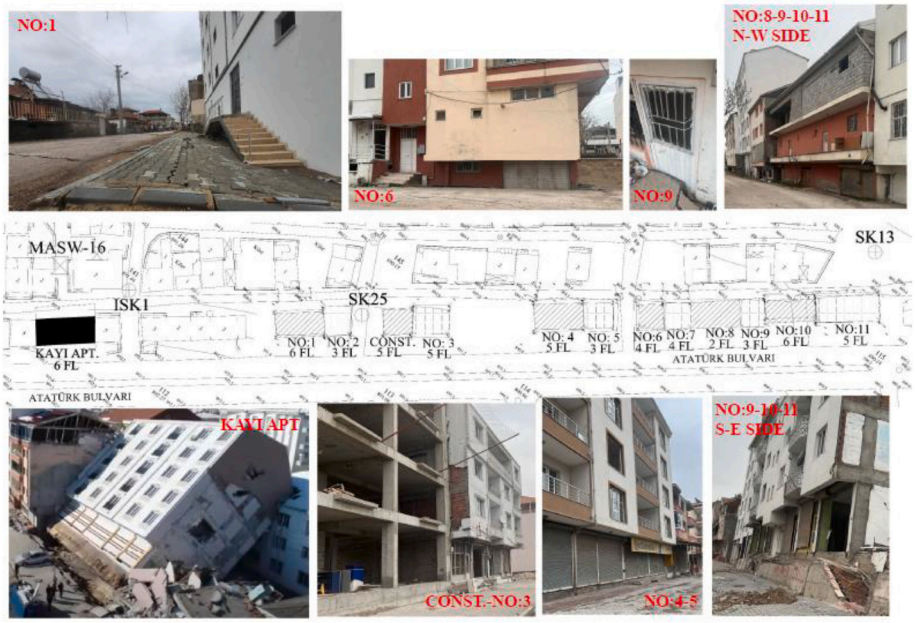

Fig. 3. Investigated buildings on Ataturk Boulevard.

visible soil bulging may be an indication that an earthquake-induced sudden loss of strength was a critical factor in triggering the failure.

3. Subsurface characterization and estimation of failure surface

In an earlier study conducted by Akıl et al. (2008), a total of 21 geotechnical boreholes were drilled at depths ranging from 15 m to 25 m in the study area. The findings indicate that the majority of the study area is composed of saturated Quaternary-age alluvial plains. These units consist predominantly of greenish light brown, brown, and poly-crystalline gravel, sand, and clay levels, with occasional silt layers. In the western part of the study area, surrounding the Gölbaşı Lake, this unit mainly consists of very fine silt and clay-sized sediments with a dark black, dark brownish, and dark grayish color, containing a significant amount of organic matter.

According to the laboratory analysis results of the retrieved 174 soil samples, 37% of the soils in the study area are coarse-grained, while 63% are fine-grained. The fine-grained soils are predominantly classified as low-plasticity clay (CL), while the coarse-grained soils are primarily classified as silty sand (SM). According to the unified soil classification, out of 174 samples, 36% belong to high-plasticity clay (CH), 24% to low-plasticity clay (CL), and 19% to clayey sand (SC). It is noteworthy that there appears to be no discernible correlation between soil types and their depth from the surface. Considering the settlement center of the district, it was observed that in the southeast of the center, along the Gölbaşı-Adıyaman highway, there is a prevalence of high-plasticity clay, while throughout the district, there is a widespread occurrence of fine-grained, low-plasticity, soft clay with occasional sand at the west (Akıl et al., 2008).

In order to assess the soil properties beneath the foundations of the structures exhibiting excessive deformations, three exploratory boreholes, including one just next to the Kayı Apartment, were drilled along

Table 1
Deformations observed in the examined buildings.

Building No.	Foundation Length L (m)	Foundation Width B (m)	Number of Floors	Total Settlement s (cm)	Differential Settlement δ (cm)
Kayı Apt.	24.00	11.00	6	***COLLAPSED***	
1	19.90	10.25	6	38–42	X
2	12.25	11.40	3	22	42–43
Const.	12.25	10.40	5	47–49	X
3	15.06	10.20	5	X	25–28
4	20.10	10.80	5	X	21
5	12.18	10.80	3	35	51–53
6	10.74	9.97	4	X	26–47
7	11.16	10.98	4	9.4	21
8	20.05	10.54	2	***NO SETTLEMENT***	
9	12.10	10.10	3	40	X
10	20.70	9.45	6	33	63–72
11	26.00	10.93	5	X	X

Note: X: Exact measurement could not be obtained.

Fig. 4. Failure of the Kayı Apartment after the earthquakes.

Ataturk Boulevard (Fig. 6). Note that existing information about subsurface conditions was also gathered, however the site characterization for Kayı Apartment failure primarily relied on the new boreholes, while the old borehole records were used as a reference. This decision was made due to concerns about the reliability of the old borehole information. Standard Penetration Tests (SPT) and Pressuremeter Tests (PMT) were performed in these boreholes to obtain disturbed and undisturbed samples for further laboratory evaluation. Shear wave velocity was also measured by MASW for a depth of about 30 m.

Fig. 7 illustrates the idealized soil profile and presents the results of in-situ and selected laboratory tests based on borehole SK-1, located adjacent to Kayı Apartment. The soil profile encountered in all the boreholes consisted primarily of a gravelly, sandy, silty clay layer, classified according to Unified Soil Classification System (USCS) predominantly as CL, with occasional classification as CH. Based on the borehole data, it was determined that the groundwater table is positioned approximately 3 m below the ground surface. The SPT N_{60} values ranged from 6 to 7 at shallow depths and increased with depth, reaching approximately 20 at a depth of about 20 m. These findings are consistent with the limit pressures (P_L) obtained from pressuremeter tests and the measured shear wave velocities (V_s), which ranged from 130 m/s in the shallow section to 200 m/s at a depth of 30 m.

Disturbed and undisturbed samples were collected to investigate the geotechnical properties of the soil, and index and classification tests including water content analysis, natural unit weight determination, sieve-hydrometer analyses, and Atterberg limit tests were performed on these samples according to relevant ASTM standards. Unconsolidated-undrained (UU) triaxial compression tests were also performed on undisturbed samples to determine the undrained strength. The laboratory test results are summarized in Table 2. Please note that the locations of the boreholes mentioned in Table 2 are given in Fig. 3.

The failure surface beneath Kayı Apartment was then identified by analyzing the observed geometry following the failure event. The approximate profile of the failure surface is depicted in Fig. 8. The variations of the undrained shear strength within the clay layer were assessed using the results obtained from the UU (undrained-unconsolidated) tests. These variations were further estimated through empirical correlations proposed by Stroud (1974) and Briaud (1992) based on SPT-N values and pressuremeter PL values, respectively. These estimations, along with the results obtained per Ladd (1991) using the average of estimations of OCR (overconsolidation ratio) derived from empirical equations suggested by Donatas et al. (2016) and Muir Wood (1990), are also illustrated in Fig. 8. It is noteworthy that the average estimated OCR values of the clay layer fall within the range of 1.8 to 2.2 between the depths of 3.0 and 12.0 m.

4. Liquefaction potential of the clay layer

While extensive research has been conducted on the liquefaction of sandy soils, there is a relative scarcity of studies focusing on the liquefaction of fine-grained soils. Initially, the susceptibility of fine-grained soils to liquefaction was not considered a significant concern due to their relatively higher cyclic strength. However, as more cases of liquefaction incidents were documented at sites with these types of soils, researchers began to recognize the importance of this issue. The accumulation of cases following the 1999 Kocaeli and Chi-Chi earthquakes served as a pivotal moment in this field, prompting researchers to propose laboratory-based or in-situ approaches for assessing the liquefaction potential of fine-grained soils. According to Seed et al. (1985), the cyclic shear stress method, commonly used to assess the liquefaction potential of clean sands and silty sands, may not be suitable for determining the liquefaction potential of fine-grained soils. In the case of fine-grained soils, the liquefaction potential is typically evaluated by considering their physical properties.

Various researchers have proposed utilizing specific physical properties of soils to determine the liquefaction potential of fine-grained soils. Parameters such as liquid limit (LL), clay content (C%), water content (w_n), and liquidity index (IL) have been identified as potential indicators of liquefaction potential. However, it should be noted that different liquefaction criteria exist in the literature, employing these parameters with different threshold values.

Two widely recognized methods, commonly referred to as the “Chinese Criterion” and the “Modified Chinese Criterion,” were introduced by Wang (1979) and Seed et al. (1983), respectively, to assess the potential for liquefaction phenomena. These methods establish specific criteria for determining whether liquefaction can occur in fine-grained soils. According to the Chinese Criterion, for a fine-grained soil to undergo liquefaction, it must meet the following conditions: the LL should be <35, the clay content should be less than or equal to 15%, and the w_n should exceed 0.9 times the liquid limit.

According to Koester (1994), liquefaction can occur in fine-grained soils if the LL is below 36, the clay content is less than or equal to 10%, and the water content exceeds 0.9 times the LL. Similarly, Finn

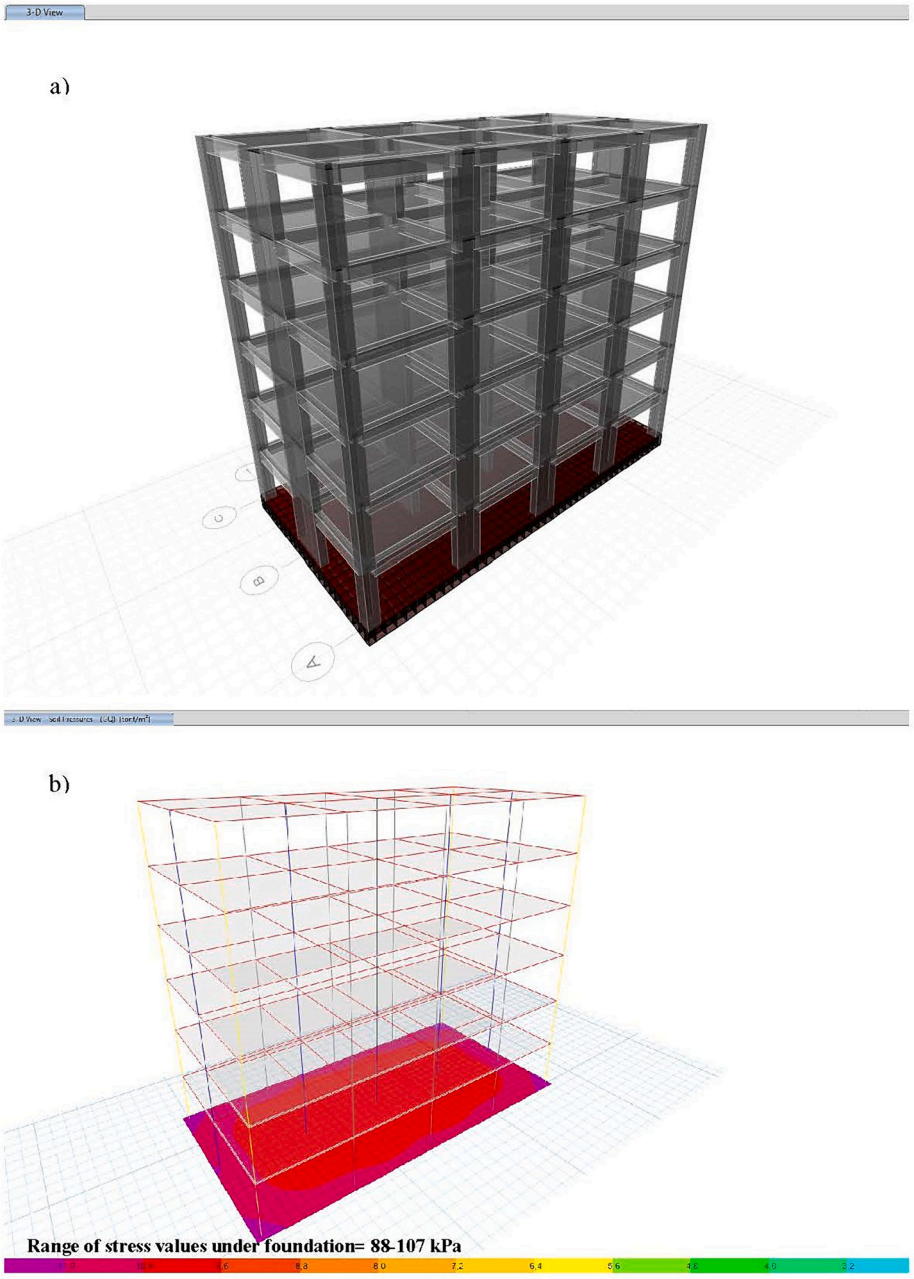

Fig. 5. a) Structural model of the Kayı Apartment; b) The distribution of bearing pressures for static loads.

et al. (1994) found that liquefaction can take place when the LL is <34 and the clay content is below or equal to 10%.

In their research, Andrews and Martin (2000) emphasized the significance of C% and LL as main parameters for distinguishing between liquefiable and non-liquefiable soils. They suggested that if the LL is <32 and the clay content is less than or equal to 10%, the soil can liquefy. Furthermore, they recommended conducting additional tests if the soil meets any of these conditions. These studies highlight the importance of considering LL, C%, and w_n as influential factors in assessing the liquefaction potential of fine-grained soils.

Seed et al. (2003) presented a method based on field observations and experimental results after earthquakes, considering the LL, plasticity index (PI), and the ratio of w_n to LI. In a more recent study by Bray and Sancio (2006), developed based on cyclic testing of silt and clay mixtures in Adapazarı, a criterion was proposed for liquefaction susceptibility based again on PI and w_n/LL. Boulanger and Idriss (2006) suggested that fine-grained soils can be considered to display clay-like characteristics if their PI exceeds 7. However, if a soil is classified as CL-ML, the PI requirement can be lowered to 5 while still maintaining consistency with the existing data. In cases where fine-grained soils do not meet these criteria, it is reasonable to assume that they exhibit sand-like behavior, meaning they are prone to liquefaction unless proven otherwise through suitable in situ and laboratory testing.

Recently Bilge and Çetin (2017) introduced a novel probabilistic criterion for evaluating the liquefaction susceptibility of silt-clay mixtures. Based on the outcomes of high-quality cyclic tests performed on undisturbed silt-clay mixtures, and by considering the wn and Atterberg Limits, this criterion provides a means to assess the potential for liquefaction in fine grained soils. According to Bilge and Çetin (2017), the soil has liquefaction potential if it satisfies the following condition:

$$0.578\ ln\ (\mathrm{PI}) - \mathrm{LI} - 0.940 < 0 \quad (1)$$

For the 33 samples tested in the laboratory the numerical value of Eq.

Fig. 6. Photographs from subsurface investigation at the study site.

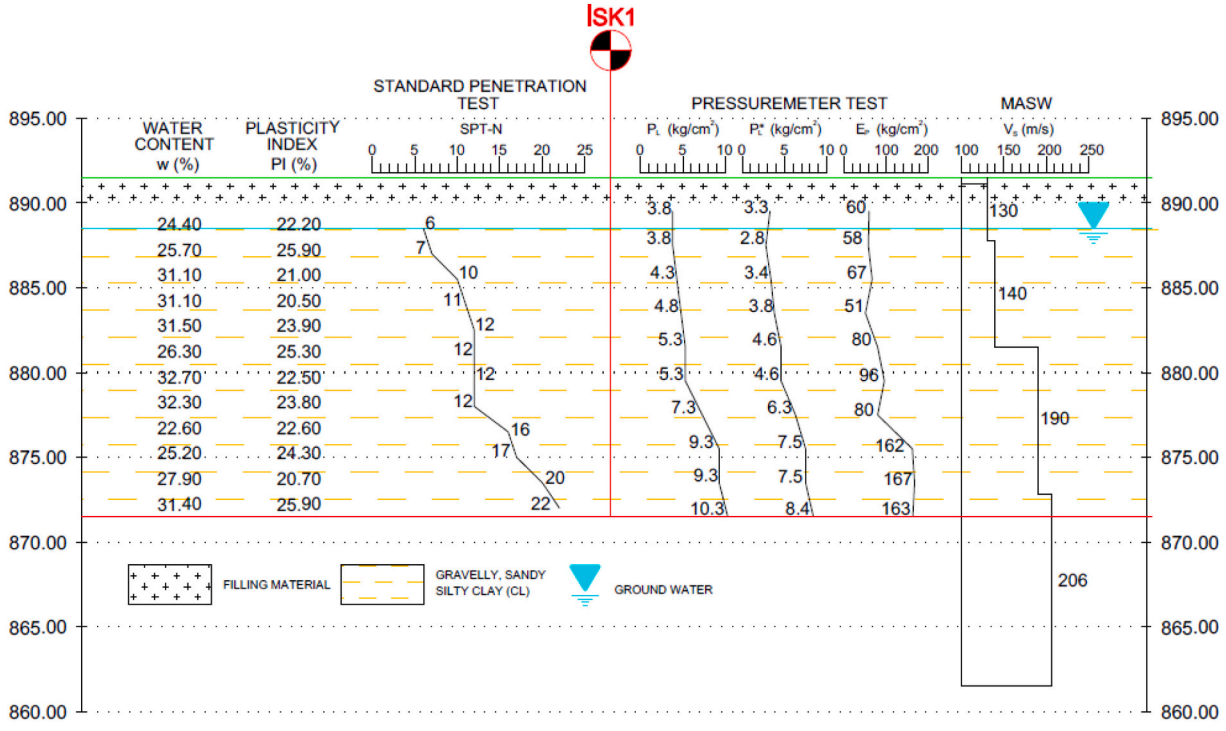

Fig. 7. Idealized soil profile and summary of in-situ test results.

1 ranges between 0.35 and 1.02 with an average of 0.73. Thus, the foundation soil has no liquefaction potential according to the criteria proposed by Bilge and Çetin (2017). On the other hand, Bilge and Çetin, 2017recommends checking for cyclic mobility if Eq. (1) is not satisfied or LI < 0.5 or PI>30, which is discussed in the next section.

In a more recent investigation conducted by Önalp et al. (2023), aimed at devising a simplified procedure for assessing the cyclic characteristics of fine-grained soils classified as ML or CL, it was concluded that soils containing 20% clay content or higher, or with a PI exceeding 24, exhibit a risk of liquefaction close to zero.

Based on the laboratory test results obtained from the exploratory borings (Table 2), none of the samples exhibit an LL below 35 or a clay content lower than 15%. The majority of the samples possess a PI exceeding 20, with a few falling within the range of 15 to 20. Additionally, the ratio of the w_n to LL ranges between 0.5 and 0.7. Consequently, based on the criteria established in the literature, it can be concluded that soil under the mat foundation Kayı Apartment, hence those of the buildings located in the study area, lacks the potential for liquefaction. But, especially considering the uncertainties or gray areas inherent in the proposed empirical criteria, a laboratory testing program was initiated to ascertain the liquefaction susceptibility of the foundation soil of Kayı Apartment.

5. Laboratory testing program

To further elaborate on the behavior of the clay layer under seismic

Table 2
Summary of laboratory test results.

Borehole No	Sample No	Depth (m)	Unit Weight (kN/m^3)	Clay Content (%)	Soil Class.	LL (%)	PL (%)	PI (%)	w_n (%)
ISK-1	PN-1	3.00	19.37	22.00	CL	49.50	27.30	22.20	24.40
	PN-2	4.50		20.00	CL	49.20	23.30	25.90	25.70
	PN-3	6.00	19.12	20.00	CL	42.30	21.30	21.00	31.10
	PN-4	7.50	19.24	23.00	CL	45.90	25.40	20.50	31.10
	PN-5	9.00		18.00	CL	46.00	22.10	23.90	31.50
	PN-6	10.50	19.17	20.00	CL	47.60	22.30	25.30	26.30
	PN-7	12.00		15.00	CL	45.80	23.30	22.50	32.70
	PN-8	13.50		18.00	CL	47.00	23.20	23.80	32.30
	PN-9	15.00		16.00	CL	44.80	22.20	22.60	22.60
	PN-10	16.50		18.00	CL	48.10	23.80	24.30	25.20
	PN-11	18.00		23.00	CL	42.40	21.70	20.70	27.90
	PN-12	19.50		19.00	CL	46.20	20.30	25.90	31.40
SK-13	SPT-1	1.50			CL	37.70	23.00	14.70	22.20
	UD-1	3.00	19.00		CL	42.00	20.00	22.00	23.60
	SPT-2	4.50			CL	39.50	18.80	20.70	22.40
	UD-2	6.00	18.60		CL	43.60	19.50	24.10	26.40
	SPT-3	7.50			GC	35.50	19.70	15.80	18.80
	SPT-4	9.00			GC	39.90	19.50	20.40	21.30
	SPT-5	10.50			GC	39.10	19.20	19.90	22.10
	UD-3	12.00	19.00		GC	35.50	20.10	15.40	20.10
	SPT-6	15.00			CH	52.30	22.50	29.80	27.30
	SPT-7	16.50			CH	55.50	22.10	33.40	26.30
	SPT-8	18.00			CH	56.20	22.40	33.80	26.70
	SPT-9	21.00			CH	58.20	23.30	34.90	26.50
SK-25	SPT-1	1.50			CL	42.20	20.40	21.80	19.30
	UD-1	3.00	18.50		CH	52.00	20.20	31.80	25.40
	SPT-2	4.50			CL	43.30	21.10	22.20	20.30
	SPT-3	6.00			CL	45.90	22.90	23.00	23.80
	UD-2	7.50	18.60		CH	54.90	19.90	35.00	24.70
	SPT-4	9.00			CL	44.40	22.30	22.10	26.30
	SPT-5	10.50			CL	44.90	22.00	22.90	29.80
	SPT-6	12.00			CL	45.20	21.30	23.90	29.50
	UD-3	13.50	18.80		CH	56.90	19.20	37.70	27.80

Note: LL: liquid limit; PL: plastic limit; PI: plasticity index; w_n: water content.

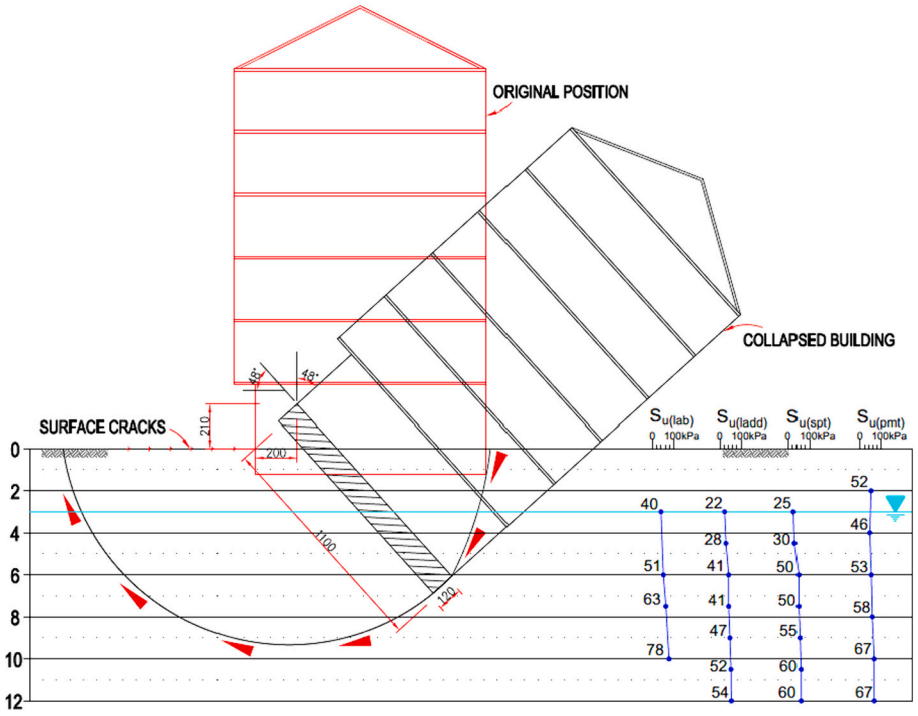

Fig. 8. Reconstructed profile of the failure surface and undrained shear strengths.

loads, a series of cyclic simple shear tests were conducted on five undisturbed clay samples obtained between depths of 3.0 m - 10.0 m from the borehole BH-1. The cyclic simple shear testing device allows for 1D, 2D, and 3D loading exerting a force of up to 10 kN, and is capable of applying either sinusoidal or random loading, where the latter is generated by inputting the displacement record of a ground motion.

During cyclic loading, a uniform sinusoidal shear strain with a frequency of 1 Hz was applied horizontally, as recommended for this type of test equipment by Chen and Loehr (2009), although this frequency is lower than that typically experienced during earthquakes. Sensitive pressure sensors located above and below the sample were used to measure excess pore water pressures that occurred during the tests. The software of the cyclic simple shear test apparatus automatically recorded all parameters during the experiment, capturing 20 readings for each cycle.

In the study, under undrained conditions, five deformation-controlled cyclic simple shear tests were performed. The tests were conducted with a maximum shear strain level of 3% and at various vertical stress values (60, 90, 120, 150 and 200 kPa). The samples can be considered to have liquefied once excess pore water pressure equal to the initial effective vertical stress was reached.

The results of experiments are presented in Fig. 9, which illustrates the hysteresis loop, demonstrating the shear stress variation with shear deformation. It is evident that the area beneath the curve does not diminish significantly as the number of cycles increases. In case the sample liquefies, the loop's area experiences a substantial decrease, resulting in a nearly straight shape.

In deformation-controlled experiments, the amplitude of the shear strain is maintained constant throughout the duration of the experiment. Fig. 9 also illustrates the variation of the applied 3% shear strain on the sample as a function of the number of cycles in this particular experiment.

Fig. 10 presents the results of a representative experiment, illustrating the variation in excess pore water pressure as a function of the number of cycles. Excess pore water pressure is a critical indicator of soil liquefaction. In case of liquefaction, it rapidly increases as sample deformation and the compaction of sand grains intensify, eventually reaching a level equal to the vertical effective stress. Following this, with the onset of liquefaction, the excess pore water pressure remains relatively constant. It is clear that no significant escalation can also be

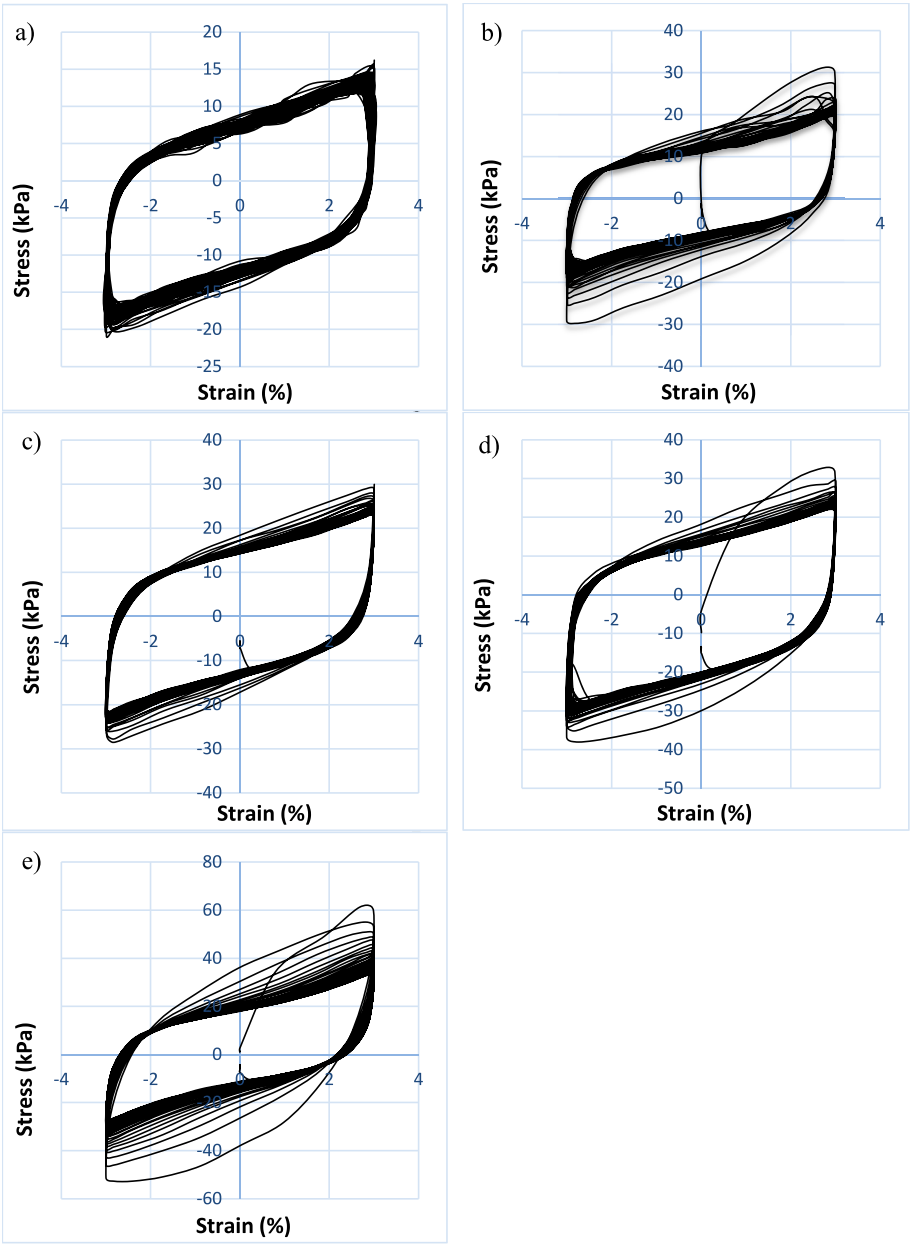

Fig. 9. Representative results from dynamic simple shear tests: a) Sample of 3.00 m; b) Sample of 4.50 m; c) Sample of 6.00 m; d) Sample of 7.50 m; e) Sample of 10.00 m.

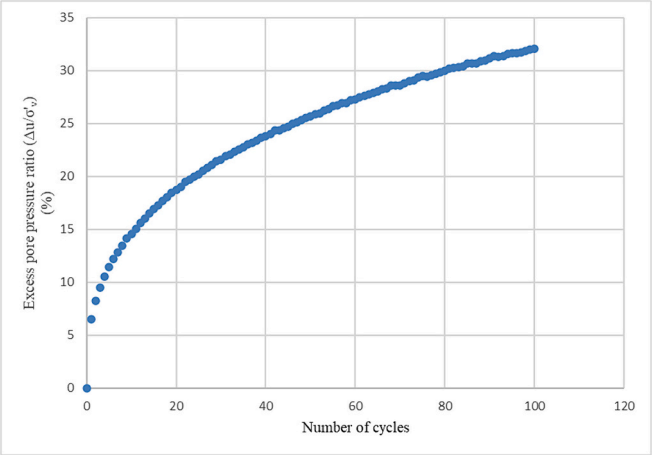

Fig. 10. Excess pore pressure ratio versus number of cycles for $\gamma = \%3$ & $\sigma'_v =$ 200 kPa.

observed in the excess pore water pressure.

The behavior observed under cyclic loading in cases where significant stiffness degradation, excess pore water pressure generation, cumulative strain accumulation, and the formation of contraction-dilation cycles occur is indicative of liquefaction triggering. However, in the conducted experiments, as revealed by the experimental results, although the specimens were subjected to 100 cycles of shear strain with an amplitude of 3%, no significant accumulation of shear strain or generation of excess pore water pressure was observed. Similarly, no significant stiffness degradation was detected.

The results of the dynamic simple shear test are consistent with the predictions of empirical liquefaction potential criteria investigated in the previous section, indicating that the foundation soil of Kayı Apartment is not susceptible to liquefaction.

6. Empirical estimation of cyclic softening of clay

Cyclic softening of clays is commonly understood as the reduction in soil stiffness and strength due to repeated cyclic loading (Ishihara, 1996; Idriss et al., 1978) and as indicated by Matasović and Vucetic (1995) it is closely linked with pore water pressure generation due to cyclic loading. Several factors, such as cyclic stress/strain amplitude, loading frequency, overconsolidation ratio (OCR), stress state, and Atterberg limits, have been found to affect the extent of degradation in stiffness or strength, as demonstrated by experimental studies (e.g., Ansal and Erken, 1989; Idriss et al., 1978; Martínez et al., 2017; Matasović and Vucetic, 1995; Vucetic and Dobry, 1988; Wijewickreme and Soysa, 2016).

Boulanger and Idriss (2007) proposed a method to evaluate the possibility of cyclic softening in fine-grained soils during earthquakes. Their approach involves examining the factor of safety in saturated clays and silts to determine the likelihood of significant strains or strength loss. Building on this work, Mejia et al. (2009) used a similar method to estimate the post-cyclic strength of these soils and applied it to evaluating dam safety. Tsai et al. (2014) proposed a strain-based procedure for assessing the degree of cyclic softening in clayey soils and incorporated this method into pseudo-static analysis for assessing slope stability and bearing capacity. Recently Tsai et al. (2022) investigated the failure of the Rixin levee during the Meinong earthquake through field exploration, laboratory testing, and numerical analysis, and illustrated that the cyclic softening of clayey soil subjected to ground shaking was considered a key factor that induced the damage.

Having established that the failure of Kayı Apartment and the excessive deformations in the nearby structures were not caused by liquefaction-induced strength loss, the focus now shifts to assessing the potential influence of cyclic softening of clay on the observed failure. To this end, as a first attempt, the strain-based procedure proposed by Tsai et al. (2014) was employed. This procedure for assessing strength softening consists of two primary steps (Tsai et al., 2014): (1) Demand Estimation, which involves estimating the shear strain amplitude and determining the equivalent number of uniform strain cycles within the soil mass. These estimates are derived from various factors such as the peak acceleration at the ground surface, seismological data, and if available, site-specific parameters, and (2) Consequence Evaluation in which, the strength softening of the soil is estimated based on the effective shear strain amplitude and the equivalent number of uniform strain cycles obtained in Step 1. The assessment takes into consideration the relationship between the applied cyclic loading and the resulting softening of the soil's strength. The estimated softened soil strength can then be used in pseudo-static or dynamic analyses of foundation bearing capacity when subjected to earthquakes.

Table 3 displays the necessary information and the outcome of the analyses. Note that due to the uncertainty in the maximum acceleration experienced during the earthquakes, analyses were performed for amax values of 0.20, 0.25, and 0.30 g. The b value, physical meaning of which represents the relative weight of different strain amplitudes to cause different levels of softening that is required for estimating the equivalent number of uniform strain cycles N_c according to Kishida and Tsai (2014), was taken as 1 as recommended by Matasović and Vucetic (1995). The results indicate that the undrained strength of saturated clay soils under the raft foundation of Kayı apartment could be reduced by approximately 11%–18% during the Kahramanmaraş EQ.

7. Estimation of cyclic softening of clay through dynamic simple shear

The cyclic strength of fine-grained soils can also be represented as a ratio of the soil's undrained shear strength (s_u). In their study, Boulanger and Idriss (2007) provided a presentation of the relationship between the ratio of cyclic shear stress to undrained shear strength and the number of uniform loading cycles (N) leading to failure, considering a peak shear strain of 3%. They examined six natural soils with OCR ranging from 1 to 4, as well as two normally consolidated tailing materials (OCR = 1). Considering the limited availability of data on cyclic strength ratios (τ_{cyc}/s_u) at N = 30 cycles (corresponding to $M_w = 7.5$), the challenging nature to establish the precise influence of various factors such as age, plasticity index (PI), soil type, OCR, and test type on the τ_{cyc}/s_u ratio was emphasized. However, their findings indicated that this ratio tends to exhibit a relatively narrow range across different natural soil types. Hence, it is recommended to adopt a $(\tau_{cyc}/s_u)_{N=30}$ ratio of 0.83, i.e., a strength loss of 17%, for natural clay-like soils under DSS (direct simple shear) loading conditions. It is important to acknowledge that as further laboratory test data is compiled, refinements to this estimation may be possible in the future. Note that the recommended value of 0.83 for the $(\tau_{cyc}/s_u)_{N=30}$ ratio is in alignment with the range of values obtained from the empirical strain-based procedure proposed by Tsai et al. (2014), as discussed in the previous section.

In order to more accurately determine the τ_{cyc}/s_u ratio for the clay layer, cyclic direct simple shear (DSS) tests were conducted on five undisturbed samples obtained from different depths: 3 m, 4.5 m, 6 m, 7.5 m, and 10 m, all extracted from borehole BH-1. Following the recommendation of Boulanger and Idriss (2007), strain-controlled tests

Table 3
Parameters used to estimate the cyclic softening of clay.

M_w	a_{max} (g)	V_s (m/s)	OCR	PI (%)	N_c	γ_{eff} (%)	Strength Loss (%)
7.7	0.20	135	1.7–2.0	20–25	60	0.20	11
	0.25				55	0.55	17
	0.30				52	0.60	18

were performed with a peak shear strain of 3% and an equivalent uniform cyclic loading frequency of 1 Hz. This approach was chosen to provide a more representative simulation of earthquake loading conditions.

It is important to note that Boulanger and Idriss (2007) defined the equivalent uniform number of cycles, N_{clay}, for $M_w = 7.5$ as 30. However, the number of equivalent uniform cycles for sand varies depending on factors such as earthquake magnitude, distance to the earthquake source, and other considerations. Liu et al. (2001) and Green and Terri (2005) have shown that the cyclic strength of clay is less affected by large changes in the number of loading cycles compared to sand. Therefore, additional refinements in terms of scaling factors are considered to be less significant for clay compared to sand. As a result, a magnitude scaling factor (MSF) of unity can be assumed for $M_w = 7.7$, and N_{clay} for the conducted tests was chosen as 30.

In Fig. 11, the relationships between τ_{cyc}/s_u and the number of uniform cycles (N) are depicted. The observed deviations in certain test curves in Fig. 11 suggest a friction in the cyclic shear test device. Thus, upon removal from the test setup, the samples underwent detailed examination. The presence of sand particles in specific samples was noted, suggesting that the additional resistances arising from these disruptions to the matrix structure might be contributing to the observed deviations. The identification of a sand content of 40% or higher in sieve analyses further bolsters this possibility.

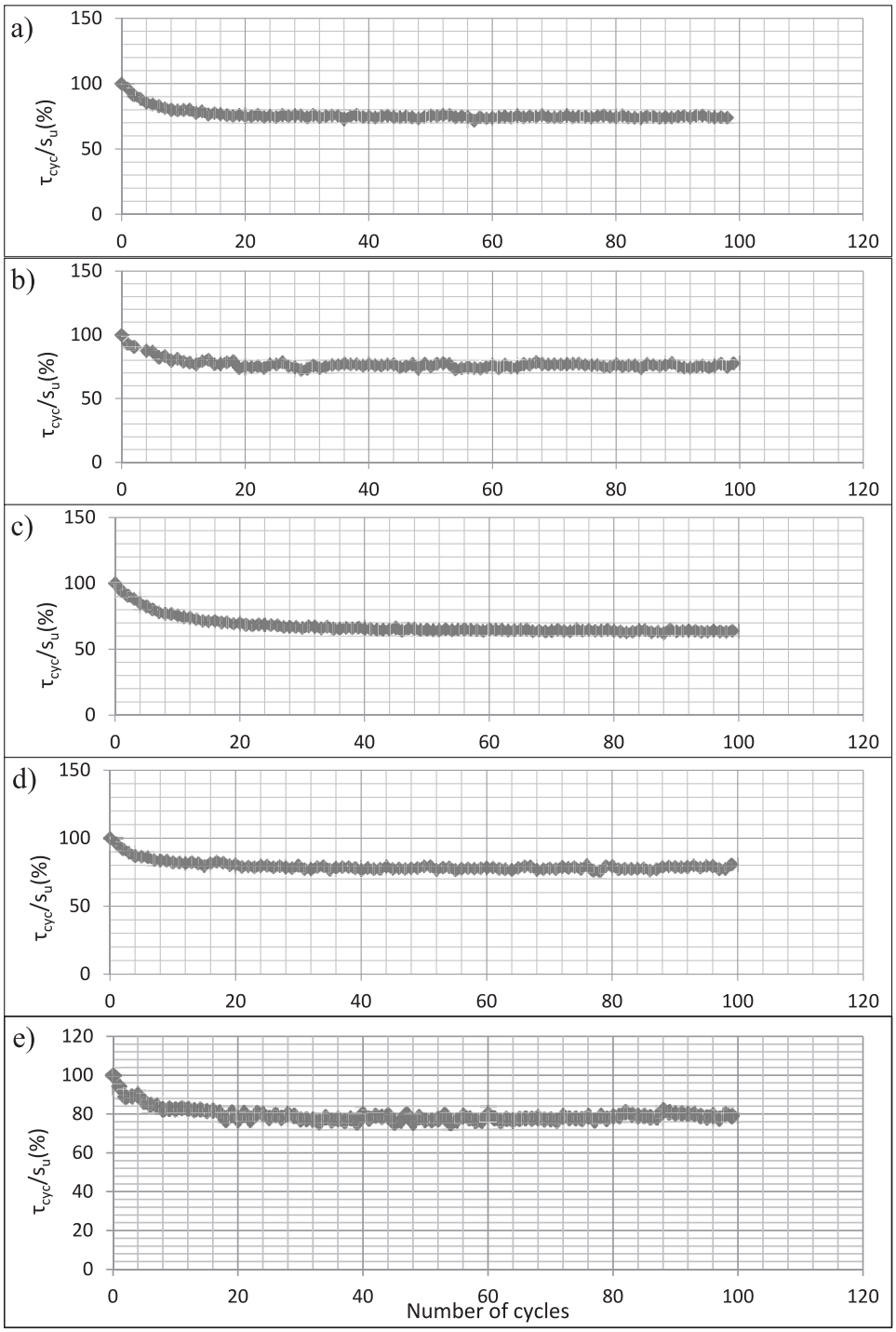

Fig. 11. τ_{cyc}/s_u ratio as a function of number of cycles: a) Sample of 3.00 m; b) Sample of 4.50 m; c) Sample of 6.00 m; d) Sample of 7.50 m; e) Sample of 10.00 m.

The obtained values for the cyclic shear to undrained shear strength ratio at 30 uniform cycles ranged from 0.81 to 0.72, with an average value of 0.77, i.e., a strength loss of 23%, for the tested samples. No distinct pattern or trend with depth was observed in these ratios. Comparing these results to the values derived from the empirical strain-based procedure suggested by Tsai et al. (2014) and Boulanger and Idriss (2007), it appears that the tested samples exhibit slightly lower ratios, indicating a relatively higher level of cyclic softening.

8. Evaluation of bearing capacity failure potential

The distribution of bearing pressures beneath the Kayı Apartment under static loading conditions, as well as during pseudo-static loading scenarios with applied base accelerations of a_{max} = 0.20 g, 0.25 g, and 0.30 g, has been analyzed and visualized in Fig. 12.

In this section, an evaluation of the bearing capacity of the foundation soils for the mat foundation of Kayı Apartment was conducted. The objective is to determine whether the established bearing capacity theory, in conjunction with appropriately selected undrained strength parameters, can accurately predict the observed performance. Based on Chu et al. (2006), three distinct conditions were considered:

1. Static bearing capacity prior to the earthquake event.
2. Static bearing capacity after the earthquake, considering the reduction in shear strengths caused by cyclically induced pore pressures.
3. Bearing capacity during intense earthquake shaking.

By examining these conditions, it was aimed to assess the effectiveness of the bearing capacity theory in capturing the actual behavior of the foundation soils under different loading scenarios.

According to the findings presented in Fig. 5b, the estimated long-term static loading on the foundation of the site is about 107 kPa. Based on the results UU and in-situ tests, as depicted in Fig. 7, the average undrained shear strength (s_u) of the upper 10 m clay layer is approximately 48 kPa. No correction for anisotropy was considered.

Applying Vesić's (1973) bearing capacity theory, the ultimate bearing capacity for the mat foundation is determined to be 275 kPa. This corresponds to a factor of safety ($FS_{pre\text{-}eq}$) of 2.6 against bearing capacity failure before the earthquake. Following the earthquake, assuming that the conditions remain unchanged, except for a reduction in the undrained shear strength by 15% to 20% on average as discussed in the previous sections, the post-earthquake factor of safety ($FS_{post\text{-}eq}$) is then estimated to range from 2.0 to 2.2.

Based on these analyses, it is concluded that no bearing capacity issues would be expected at the site either prior to or after the earthquake without any change in the soil strength. This conclusion is consistent with reports from local residents, who have observed no further settlement of the foundation following the earthquake.

During the earthquake, the modification of the bearing capacity factor N_c to N_{ce} is necessary to account for inertial forces within the soil mass, which is commonly referred to as the kinematic interaction effect on bearing capacity. Studies by Pecker (1996) and Mylonakis et al. (2002) have indicated that this effect is minimal for bearing capacity analysis of undrained clays, and thus any change in the bearing capacity factor was not considered in the analyses conducted herein.

However, in the analysis of bearing capacity, it is important to consider the inclination of the load acting on the footing. Based on the outputs of the structural analyses the load inclination factor §ci, according to Vesić's (1973) approach, is 0.84, 0.81, 077 for pseudo-acceleration values of 0.20 g, 0.25 g, and 0.30 g, respectively. Additionally, as can be seen from Fig. 12, the maximum bearing stress during the earthquake is increased to about 160–180 kPa under these accelerations. The factor of safety during earthquakes (FS_{eq}) is then determined to be between 1.2 and 1.4, depending on the peak acceleration experienced, without considering any cyclic softening or any increase due to loading rate in the undrained shear strength. Contrary to the observations at the site, this FSeq value still indicates a low probability of bearing capacity failure, unless there is a simultaneous decrease in clay shear strength caused by the earthquake and the generation of pore pressure, known as cyclic softening.

When the average undrained shear strength of clay is decreased by 15% to 20% due to cyclic softening, the FS_{eq} values are further diminished to a narrow range of approximately 0.9 to 1.1 as a function of amax. These values indicate strongly that the observed foundation failure was indeed a bearing capacity failure resulting from both earthquake-induced reductions in clay strength, i.e., cyclic softening, and increased bearing pressure demands exerted on the foundation during seismic loading.

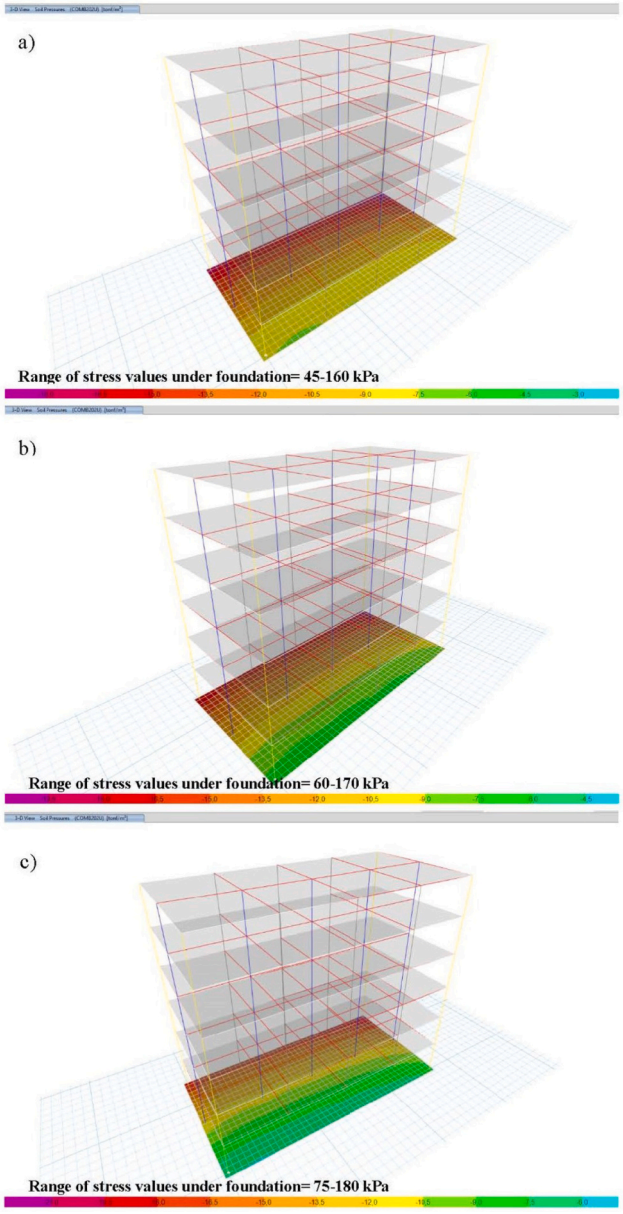
a)
Range of stress values under foundation= 45-160 kPa
b)
Range of stress values under foundation= 60-170 kPa
c)
Range of stress values under foundation= 75-180 kPa

Fig. 12. The distribution of bearing pressures for: a) 0.20 g; b) 0.25 g; c) 0.30 g.

9. Conclusions

In this study, the excessive settlements observed at buildings along Ataturk Boulevard in Golbasi district during the Kahramanmaras Earthquakes were investigated, with a primary focus on the toppling of Kayı Apartment. The foundation failure of Kayı Apartment received

considerable public attention and was initially attributed to liquefaction. Immediately following the earthquake, a reconnaissance was conducted to provide a preliminary assessment of the failure mechanism. Subsequently, additional field investigations and laboratory tests were carried out to characterize the soil conditions at the foundation site. Based on this information, dynamic simple shear testing, as well as liquefaction and bearing capacity analyses were performed to gain a deeper understanding of the underlying failure mechanism.

The failure of Kayı Apartment's foundation cannot be attributed to liquefaction since it has been demonstrated through literature-based approaches and dynamic simple shear testing that the clayey soil present in the foundation does not possess the potential for liquefaction. Instead, findings from both laboratory testing and empirical approaches indicated the potential for significant strength loss in a saturated clay foundation during the earthquake. The cyclic softening of clayey soil under seismic loading was considered a key factor contributing to the observed damage. According to Tsai et al. (2014) and dynamic shear testing, the strength of the foundation soil was estimated to have decreased up to approximately 18% and 23% due to cyclic softening, respectively, during the Kahramanmaras Earthquakes. Consequently, the factor of safety against bearing capacity failure under undrained conditions approached slightly under unity for the apartment building, aligning with the observed damage to the structure. The calculated FS (Factor of Safety) value, which is close to one for the six-story apartment, provides an explanation for how the neighboring lower-rise structures were able to withstand the earthquakes with excessive deformations without experiencing a complete failure in bearing capacity.

Due mainly to the scarcity of documented failures resulting from cyclic softening, conventional design practices often concentrate on assessing soil strength loss under dynamic conditions by primarily addressing liquefaction potential. The potential for cyclic softening and its associated consequences are typically overlooked in routine evaluations. However, the results and assessments presented in this study demonstrate that neglecting the phenomenon of cyclic softening in clayey soils can lead to highly destructive outcomes during earthquakes. Hence, this significant case history underscores the critical necessity of integrating the potential strength loss induced by cyclic softening during seismic events into geotechnical design considerations.

CRediT authorship contribution statement

İ. Tonyalı: Writing – original draft, Investigation, Formal analysis, Data curation, Conceptualization. **S.O. Akbas:** Writing – original draft, Supervision, Methodology, Conceptualization. **T. Beyaz:** Investigation, Data curation. **K. Kayabalı:** Supervision, Resources, Project administration. **C. Gokceoglu:** Writing – review & editing, Methodology, Conceptualization.

Declaration of competing interest

The authors declare that they have no known competing financial interests or personal relationships that could have appeared to influence the work reported in this paper.

Data availability

Data will be made available on request.

References

Akıl, B., Akpınar, K., Üçkardeşler, C., Araz, H., Sağlam, M., Uran, Ş.B., 2008. Doğu Anadolu fay zonu üzerinde yer alan Gölbaşı (Adıyaman) Yerleşim alanindaki zeminlerin jeoteknik özellikleri ve değerlendirilmesi [Evaluation of settlement suitability of Gölbaşi (Adiyaman) town, located on the east anatolian fault zone]. Türk. Jeol. Bül. 51, 43–57.

Andrews, D.C.A., Martin, G.R., 2000. Criteria for liquefaction of silty soils. In: Proc., 12th World Conf. On Earthquake Engineering. https://www.iitk.ac.in/nicee/wcee/article/0312.pdf (accessed 15 May 2023).

Ansal, A.M., Erken, A., 1989. Undrained behavior of clay under cyclic shear stresses. J. Geotech. Eng. 115, 968–983. https://doi.org/10.1061/(ASCE)0733-9410(1989)115:7(968).

Bilge, H., Çetin, K.Ö., 2017. Silt-kil karişimi zeminlerin sivilaşma potansiyellerinin belirlenmesi. 4. Uluslararası Deprem Mühendisliği ve Sismoloji Konferansı, Eskişehir, pp. 11–13.

Boulanger, R.W., Idriss, I.M., 2006. Liquefaction susceptibility criteria for silts and clays. J. Geotech. Geoenviron. Eng. 132, 1413–1426. https://doi.org/10.1061/(ASCE)1090-0241(2006)132:11(1413).

Boulanger, R.W., Idriss, I.M., 2007. Evaluation of cyclic softening in silts and clays. J. Geotech. Geoenviron. Eng. 133, 641–652. https://doi.org/10.1061/(ASCE)1090-0241(2007)133:6(641).

Bray, J.D., Sancio, R.F., 2006. Assessment of the liquefaction susceptibility of fine-grained soils. J. Geotech. Geoenviron. Eng. 132, 1165–1177. https://doi.org/10.1061/(ASCE)1090-0241(2006)132:9(1165).

Briaud, J.L., 1992. The Pressuremeter. A. A. Balkema, Rotterdam, Netherlands.

Chen, C.W., Loehr, J.E., 2009. Undrained and drained triaxial tests of fiber-reinforced sand. Geosynthetics in Civil and Environmental Engineering: Geosynthetics Asia 2008 Proceedings of the 4th Asian Regional Conference on Geosynthetics in Shanghai, China.

Chu, D.B., Stewart, J.P., Leslie Youd, T., Chu, B.L., 2006. Liquefaction-induced lateral spreading in near-fault regions during the 1999 Chi-Chi, Taiwan earthquake. J. Geotech. Geoenviron. Eng. 132, 1549–1565. https://doi.org/10.1061/(ASCE)1090-0241(2006)132:12(1549).

Chu, D.B., Stewart, J.P., Boulanger, R.W., Lin, P.S., 2008. Cyclic softening of low-plasticity clay and its effect on seismic foundation performance. J. Geotech. Geoenviron. Eng. 134, 1595–1608. https://doi.org/10.1061/(ASCE)1090-0241(2008)134:11(1595).

Donatas, U., Ieva, L., Domas, G., 2016. Over consolidation ratio determination of cohesive soil. Historical experience and challenges of geotechnical problems in Baltic Sea region. In: Proceedings of 13th Baltic Sea Geotechnical Conference, Lithuanian Geotechnical Society, Lithuania.

EERI, 2023. Türkiye Earthquakes: Report on Geoscience and Engineering Impacts. GEER Associaon Report 082 https://learningfromearthquakes.org/images/2023_02_06_nurdagi_turkey/GEER_2023_Turkey_Earthquake_FullReport_ReducedSize.pdf (accessed 25 June 2023).

Finn, W.D., Ledbetter, R.H., Guoxi, W., 1994. Liquefaction in silty soils: design and analysis. In: Prakash, S., Dakoulas, P. (Eds.), Ground Failures under Seismic Conditions. ASCE, New York, pp. 51–76.

Gratchev, I.B., Sassa, K., Osipov, V.I., Sokolov, V.N., 2006. The liquefaction of clayey soils under cyclic loading. Eng. Geol. 86, 70–84. https://doi.org/10.1016/j.enggeo.2006.04.006.

Green, R.A., Terri, G.A., 2005. Number of equivalent cycles concept for liquefaction evaluations—Revisited. J. Geotech. Geoenviron. Eng. 131, 477–488. https://doi.org/10.1061/(ASCE)1090-0241(2005)131:4(477).

Idriss, I.M., Dobry, R., Singh, R.D., 1978. Nonlinear behavior of soft clays during cyclic loading. J. Geotech. Eng. Div. 12, 1427–1447. https://doi.org/10.1061/AJGEB6.0000727.

Ishihara, K., 1996. Soil Behaviour in Earthquake Geotechnics. Clarendon Press, Oxford.

Kayabasi, A., Gokceoglu, C., 2018. Liquefaction potential assessment of a region using different techniques (Tepebasi, Eskisehir, Turkey). Eng. Geol. 246, 139–161. https://doi.org/10.1016/j.enggeo.2018.09.029.

Kishida, T., Tsai, C.C., 2014. Seismic demand of the liquefaction potential with equivalent number of cycles for probabilistic seismic hazard analysis. J. Geotech. Geoenviron. Eng. 140, 04013023.

Koester, J.P., 1994. The influence of fines type and content on cyclic strength. In: Prakash, S., Dakoulas, P. (Eds.), Ground Failures Under Seismic Conditions. ASCE, New York, pp. 17–33.

Ladd, C.C., 1991. Stability evaluation during staged construction. J. Geotech. Eng. 117, 540–615. https://doi.org/10.1061/(ASCE)0733-9410(1991)117:4(540).

Liu, A.H., Stewart, J.P., Abrahamson, N.A., Moriwaki, Y., 2001. Equivalent number of uniform stress cycles for soil liquefaction analysis. J. Geotech. Geoenviron. Eng. 127, 1017–1026. https://doi.org/10.1061/(ASCE)1090-0241(2001)127:12(1017).

Martin, J.R., Olgun, C.G., Mitchell, J.K., Durgunoglu, H.T., 2004. High-modulus columns for liquefaction mitigation. J. Geotech. Geoenviron. Eng. 130, 561–571.

Martínez, E., Patiño, H., Galindo, R., 2017. Evaluation of the risk of sudden failure of a cohesive soil subjected to cyclic loading. Soil Dyn. Earthq. Eng. 92, 419–432. https://doi.org/10.1016/j.soildyn.2016.10.017.

Matasović, N., Vucetic, M., 1995. Generalized cyclic-degradation-pore-pressure generation model for clays. J. Geotech. Eng. 121, 33–42. https://doi.org/10.1061/(ASCE)0733-9410(1995)121:1(33).

Mejia, L., Wu, J., Feldsher, T., Yiadom, A., 2009. Re-evaluation of the seismic stability of Chabot Dam. In: Proceedings of the Annual US Society on Dams Conference, USSD.

Mylonakis, G., Gazetas, G., Nikolaou, S., Chauncey, A., 2002. Development of Analysis and Design Procedures for Spread Footings. Multidisciplinary Center for Earthquake Engineering Research, New York.

Önalp, A., Bol, E., Özocak, A., Sert, S., Ural, N., Arel, E., 2023. Influence of index properties on the cyclic failure of fine-grained soils. Eng. Geol. 317, 107056 https://doi.org/10.1016/j.enggeo.2023.107056.

Pecker, A., 1996. Seismic bearing capacity of shallow foundations. In: State-of-the-Art: 11th World Conference on Earthquake Engineering, Acapulco, Mexico.

Şaroğlu, F., Emre, Ö., Boray, A., 1987. Türkiye'nin Diri Fayları ve Depremsellikleri. MTA. Jeoloji Etüdleri Dairesi Başkanlığı, Ankara.

Seed, H.B., Idriss, I.M., Arango, I., 1983. Evaluation of liquefaction potential using field performance data. J. Geotech. Eng. 109, 458–482. https://doi.org/10.1061/(ASCE)0733-9410(1983)109:3(458).

Seed, H.B., Tokimatsu, K., Harder, L.F., Chung, R.M., 1985. Influence of SPT procedures in soil liquefaction resistance evaluations. J. Geotech. Eng. 111, 1425–1445. https://doi.org/10.1061/(ASCE)0733-9410(1985)111:12(1425).

Seed, R.B., Cetin, K.O., Moss, R.E.S., Kammerer, A.M., Wu, J., Pestana, J.M., Riemer, M. F., Sancio, R.B., Bray, J.D., Kayen, R.E., 2003. Recent advances in soil liquefaction engineering: a unified and consistent framework. In: Proceedings of the 26th Annual ASCE Los Angeles Geotechnical Spring Seminar, Long Beach, CA.

Stroud, M.A., 1974. The standard penetration test in insensitive clays and soft rocks. In: Proceedings of the 1st European Symposium on Penetration Testing, pp. 367–375.

Tsai, C.C., Hashash, Y.M., 2009. Learning of dynamic soil behavior from downhole arrays. J. Geotech. Geoenviron. Eng. 135, 745–757. https://doi.org/10.1061/(ASCE)GT.1943-5606.0000050.

Tsai, C.C., Mejia, L.H., Meymand, P., 2014. A strain-based procedure to estimate strength softening in saturated clays during earthquakes. Soil Dyn. Earthq. Eng. 66, 191–198. https://doi.org/10.1016/j.soildyn.2014.07.003.

Tsai, C.C., Yang, Z.X., Chung, M.H., Hsu, S.Y., 2022. Case study of large-scale levee failures induced by cyclic softening of clay during the 2016 Meinong earthquake. Eng. Geol. 297, 106518.

Vesić, A.S., 1973. Analysis of ultimate loads of shallow foundations. J. Soil Mech. Found. Div. 99, 45–73. https://doi.org/10.1061/JSFEAQ.0001846.

Vucetic, M., Dobry, R., 1988. Degradation of marine clays under cyclic loading. J. Geotech. Eng. 114, 133–149. https://doi.org/10.1061/(ASCE)0733-9410(1988)114:2(133).

Wang, W., 1979. Some Findings in Soil Liquefaction. Water Conservancy and Hydroelectric Power Scientific Research Institute, Beijing, China.

Wijewickreme, D., Soysa, A., 2016. Stress–strain pattern–based criterion to assess cyclic shear resistance of soil from laboratory element tests. Can. Geotech. J. 53, 1460–1473. https://doi.org/10.1139/cgj-2015-0499.

Wood, D.M., 1990. Soil Behaviour and Critical State Soil Mechanics. Cambridge University Press, Cambridge.

Xu, C., Feng, C., Du, X., Zhang, X., 2020. Study on liquefaction mechanism of saturated sand considering stress redistribution. Eng. Geol. 264, 105302 https://doi.org/10.1016/j.enggeo.2019.105302.